A Numerical Study of the Propagation of Topographic Rossby Waves*

PING-TUNG SHAW AND CHERN-YUAN PENG

Institute of Oceanography, National Taiwan University, Taipei, Taiwan, R.O.C.

(Manuscript received 10 February 1986, in final form 19 September 1986)

ABSTRACT

The propagation of linear barotropic Rossby waves is investigated numerically over a one-dimensional topography similar to the continental rise and slope. A point source is used to generate waves with periods from 4 to 36 days. The resulting distribution of streamfunction and kinetic energy density is examined.

The results show that the propagation of topographic Rossby waves depends strongly on the wave period. Over the continental rise, waves are generated mainly by low-frequency disturbances at periods of about a month. In addition, the continental slope is a good insulator to these waves. Therefore, deep ocean circulation will not influence motions on the continental shelf. At 36 and 15 days, the steep continental slope is a wave guide, and regions of high energy density generated by local sources may be found. Energy of 36-day waves over the continental shelf cannot penetrate the steep slope. Although waves of periods shorter than a week may reach the lower slope, these waves are trapped by the coast, similar to shelf waves. Consequently, the deep ocean circulation is hardly influenced by motions on the shelf and slope.

1. Introduction

Topographic Rossby waves (TRWs) with periods from a week to a month have long been observed over the continental rise at site D (39.10°N, 70.00°W) south of the New England coast (Thompson, 1971, 1977; Thompson and Luyten, 1976). Hogg (1981) has suggested that these waves may be generated by disturbances in the Gulf Stream or by the instability of mean flow on the lower rise. Over the continental slope, TRWs have also been observed. Louis et al. (1982) found bursts of TRWs for three or four cycles with periods between 10 and 23 days on the outer continental shelf and slope off Nova Scotia. They suggested that these waves were generated by the Gulf Stream rings over the slope. Recently, mooring measurements over the continental slope south of Cape Cod show that energy of TRWs propagates shoreward from the continental rise onto the lower slope (Shaw and Csanady, 1987).

Propagation of plane topographic Rossby waves of infinite along-isobath extent has been studied by several authors. Rhines (1969) showed that a small step in the ocean was effective in reflecting incident barotropic Rossby waves. Later, using a barotropic Rossby wave model over large topographic variations, Kroll and Niiler (1976) found that high energy transmission across the slope–rise junction occurred only for incoming deep ocean waves of certain wavelengths. Ou and Beardsley (1980) studied numerically the propagation of TRWs in a uniformly stratified ocean over a realistic topography. Their results showed similar dependence of onshore energy flux on the wavelength. In these models, energy flux is uniform along isobaths, and no wave turning is possible. Incoming wave energy has to be reflected, except in the case when the slope width is an integral number of the half wavelengths, i.e., the Ramshauer effect (Rhines, 1969). Consequently, the continental slope is a barrier to most TRWs from the deep ocean, and reflected waves should be observed on the rise (Rhines, 1971). Nevertheless, observations at site D have shown that TRWs propagate shoreward onto the upper continental rise and lower slope with little reflection (Thompson, 1971; Shaw and Csanady, 1987). The discrepancy between model results and observations can be resolved by taking wave refraction into consideration.

One way to study wave refraction is to calculate ray paths of waves. Hogg (1981) used WKB theory to trace ray paths of TRWs and found considerable turning of waves over the continental rise near site D. However, the length scale of the continental slope is about 50 km, while Louis et al. (1982) have observed that the cross-isobath wavelengths are 175 km. WKB approximation breaks down when the topography varies rapidly over a wavelength (e.g., Bender and Orszag, 1978). Asymptotic approximations such as the WKB method are not applicable to the steep continental slope.

Coefficients of the governing equation for TRWs will vary slowly in a wavelength if a smooth topography is used. Kroll (1979) joined two exponential profiles at the shelf break to have constant coefficients in the gov-

* Contribution No. 266 from Institute of Oceanography, National Taiwan University.

erning wave equation. He then solved the equation asymptotically to study the wave propagation from a point source in the deep ocean. He found that the amount of energy reaching a particular point on the shelf depended on wave frequency as a result of wave refraction. Louis and Smith (1982) used a parabola to approximate the continental slope to study the barotropic TRWs generated by a point source. They explained the absence of reflected waves as a result of ray refraction and bottom friction. Although local topography of the slope may be well represented by such approximations, it is not possible to fit the entire region from the shelf to the rise with a smooth analytic function. The bottom slope changes one order of magnitude across both the shelf break and the slope/rise junction. The rapid topographic variations should not be overlooked in studying energy transmission from the continental rise onto the slope and shelf.

If there is an onshore component of group velocity and no friction, deep ocean waves will eventually reach the shelf break at an infinite coast. However, if the onshore component of the group velocity is small, waves may not reach the shelf in a finite alongshore distance. The problem is "Given a realistic frictional coefficient and limited alongshore extent, will waves reach the shelf before they are dissipated?" Recently, Peng and Shaw (1986) studied numerically the low-frequency (period at 40 days) TRWs generated by a point source over a two-dimensional realistic topography. They found that waves turned very effectively to the direction of isobaths over a steep continental slope. In this paper, we will extend the above study to higher frequencies and study how much energy can reach the shallow waters before being dissipated by bottom friction. The bottom profile resembles the offshore variation of topography from the continental shelf to the rise in the ocean. The insulating effect of the slope is studied in periods ranging from a few days to about a month. We will examine the strength of TRWs generated by a source at various locations.

2. Numerical method

The equations governing motion of barotropic Rossby waves over topography are

$$\frac{\partial u}{\partial t}-fv=-\frac{1}{\rho}\frac{\partial p}{\partial x}-\frac{1}{h}\frac{\tau_b^{(x)}}{\rho} \tag{1}$$

$$\frac{\partial v}{\partial t}+fu=-\frac{1}{\rho}\frac{\partial p}{\partial y}-\frac{1}{h}\frac{\tau_b^{(y)}}{\rho} \tag{2}$$

$$\frac{\partial (hu)}{\partial x}+\frac{\partial (hv)}{\partial y}=0 \tag{3}$$

where u and v are the velocity components in the x- and y-directions; $\tau_b^{(x)}$ and $\tau_b^{(y)}$ are the bottom stress components; and h is the bottom depth. Other symbols have the usual meaning. Because the bottom topography is more important than the variation in f, the β-effect is neglected. We have also used the rigid-lid approximation in the continuity equation. From (3), a transport streamfunction ψ can be defined as

$$hu=-\frac{\partial \psi}{\partial y} \tag{4}$$

$$hv=+\frac{\partial \psi}{\partial x}. \tag{5}$$

Furthermore, we assume a linear bottom stress proportional to the near-bottom geostrophic velocity with a proportionality constant r. The vorticity equation obtained from (1) and (2) is

$$\nabla_h^2\left(\frac{\partial \psi}{\partial t}\right)-\left(\frac{\partial^2 \psi}{\partial x \partial t}S_x+\frac{\partial^2 \psi}{\partial y \partial t}S_y\right)-fS_y\frac{\partial \psi}{\partial x}+fS_x\frac{\partial \psi}{\partial y}$$
$$=-\frac{r}{h}\nabla_h^2\psi+\frac{2r}{h}S_x\frac{\partial \psi}{\partial x}+\frac{2r}{h}S_y\frac{\partial \psi}{\partial y}+F \tag{6}$$

where $S_x = h^{-1}(\partial h/\partial x)$, $S_y = h^{-1}(\partial h/\partial y)$ and ∇_h^2 is the horizontal Laplacian. In (6), we have added a vorticity source F of the dimension of the wind stress curl to represent the unknown mechanisms of Rossby wave generation on the continental slope and rise.

Time integration of (6) can be performed numerically. If forcing is oscillatory in time, the solution will consist of a wave part and a transient part (e.g., Gill, 1982, Chapter 7). When forcing persists long enough, the transient part dies out. The remaining wave solution is the same as that obtained by assuming a solution of sinusoidal time dependence. Wang (1980), among others, has successfully solved the equation for shelf wave scattering by this substitution. This approach will greatly reduce the computation in a time-stepping problem and will be used here.

When forcing is at a single frequency, $F = F_0 \exp(-i\sigma t)$, the solution of (6) is of the form

$$\psi(x, y, t)=\phi(x, y)e^{-i\sigma t}. \tag{7}$$

Substituting (7) into (6), we have

$$\left(1+\frac{ir}{\sigma h}\right)\nabla_h^2\phi-\left(1+\frac{2ir}{\sigma h}\right)S_x\frac{\partial \phi}{\partial x}-\left(1+\frac{2ir}{\sigma h}\right)S_y\frac{\partial \phi}{\partial y}$$
$$-\frac{if}{\sigma}\left(S_y\frac{\partial \phi}{\partial x}-S_x\frac{\partial \phi}{\partial y}\right)=\frac{iF_0}{\sigma}. \tag{8}$$

Equation (8) is solved numerically. The finite difference equation is obtained by using a centered-difference scheme and is of the block tridiagonal form. It can be solved by the method of Lindzen and Kuo (1969).

Without any knowledge of the generation of TRWs, a point source might be a reasonable choice. The spatial Fourier transform of the forcing function is a broadband of wavenumbers. With broadband spatial variations, the dependence of energy transmission on wavelengths (e.g., Kroll, 1979) will show up in the results if

there is one. Louis and Smith (1982) and many others have used point sources to study the wave propagation. Therefore, a point source is used to generate TRWs in this model. To ensure that variations of the forcing scale do not alter our results, we have changed the size of the forcing area in the model. No significant difference in results is found.

In this study, bottom topography is a function of the offshore coordinate only and is similar to the one at site D (Fig. 1). The 200 and 2000 m isobaths represent the shelf break and the slope–rise junction, respectively. The study area is a 300 km × 300 km square (see Fig. 2). A coast is located along the upper boundary with the x-axis offshore and y-axis alongshore. The origin is at the upper left corner of the study region. The grid sizes are 5 km in x and 12.5 km in y. A localized source over a square of 3 × 3 grid points is used to generate TRWs. A value of F_0 is chosen to be 10^{-7} m s^{-2} to have realistic velocity of the order 0.1 m s^{-1} in the study region. A bottom frictional coefficient, $r = 5 \times 10^{-4}$ m s^{-1}, is used. This is the typical value observed on the continental shelf (e.g., Winant and Beardsley, 1979).

Boundary conditions are important in solving the elliptic equation (8). There are two types of boundaries in this problem. At the coast, the no normal flow condition is specified. On the deep ocean side, an open boundary condition is needed. Ideally, a radiation condition such as the one used by Wang (1980) should be applied to the open boundary. However, the energy spectrum in our study is continuous rather than discrete as in Wang's model, and the radiation condition is difficult to comply with. To simplify the problem, we use $\psi = 0$ at these boundaries. Results show that friction will damp out most reflected waves at the boundaries. For waves of a few days period on the shelf, some wave reflection may be found on the slope. However, the overall picture is not altered. We have also used a sponge layer at the open boundaries to eliminate the reflected waves. Inside the sponge layer, r increases linearly from 5×10^{-4} m s^{-1} in the interior to 5×10^{-3} m s^{-1} at the boundary. The thickness of the sponge layer is 50 km. However, its presence is not very significant. As long as a large amount of wave energy does not reach the boundary, as is the case in this study, the results should be meaningful.

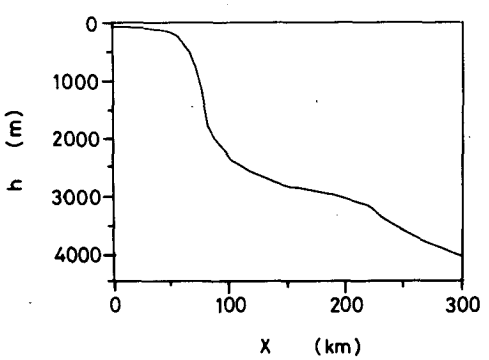

FIG. 1. Bottom topography used in the model.

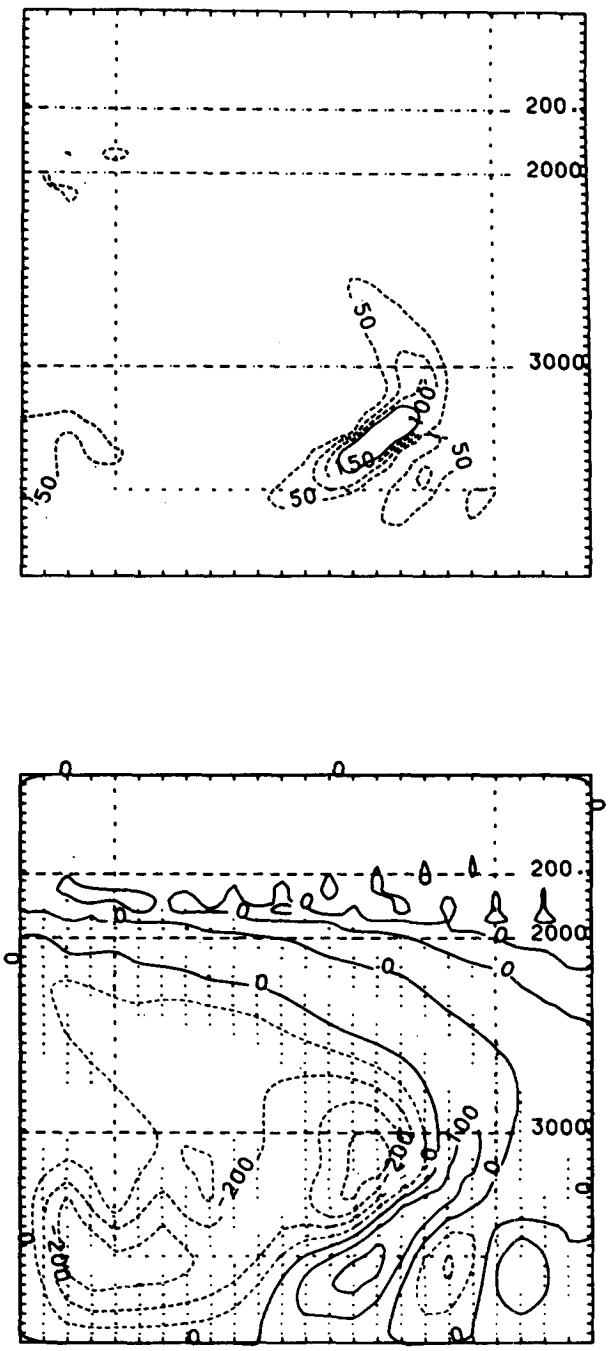

FIG. 2. Kinetic energy density (upper panel) and transport streamfunction (lower panel) of topographic waves generated by a source on the lower rise at 36 days. Contour interval is 50×10^{-5} (dashed lines) and 200×10^{-5} m^2 s^{-2} (solid lines) in the energy plot and 100×10^4 m^3 s^{-1} in the transport streamfunction plot. Isobaths at 200, 2000, and 3000 m are shown. Vectors represent velocity.

3. Numerical results

Equation (8) is solved for the streamfunction at seven periods, 4, 5, 6, 7, 10, 15 and 36 days, to study the propagation of TRWs. Examples are discussed in three period ranges: 4–7, 10–15 and 36 days. Kinetic energy density and the transport of waves are examined for sources at different offshore locations. Depth-integrated kinetic energy averaged along isobaths is used to demonstrate the offshore energy partition.

a. Forcing from the lower rise (x = 205 km, y = 187.5 km)

Energy density and the streamfunction of TRWs at a period of 36 days are shown in Fig. 2. The source is located near the high energy center in the upper panel. Waves propagate from the source toward the $-y$ direction along two paths: one to the upper rise and one to the deep ocean. Wave energy is higher along the latter path, where the bottom slope becomes greater (Fig. 1). It seems that energy tends to propagate toward the region of steep bottom slope. The current and the volume transport in the lower panel of Fig. 2 are confined in the deep waters.

Depth-integrated kinetic energy at 36, 15 and 4 days is shown in Fig. 3. Wave energy on the rise is reduced drastically when the period of the source decreases to 4 days. Also, onshore energy transmission on the slope varies with wave periods. At 36 days, energy decreases sharply across the slope from the rise while energy at 15 days penetrates farther up the slope. In spite of the shallow depth of the shelf, kinetic energy density on the shelf remains small at these periods. Therefore, the continental slope is an excellent insulator to the energy transmission at a time scale longer than 10 days. For shorter periods, the efficiency of the slope as an insulator decreases. At 4 days, energy in the water column is about the same across the slope, and the slope can no longer block energy transmission. Energy density may be large on the shelf because of the shallow depth.

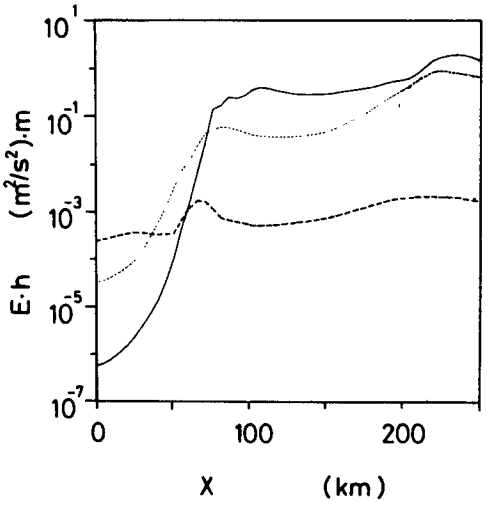

FIG. 3. Depth-integrated kinetic energy averaged over isobaths. The solid, dotted, and dashed lines represent energy at 36, 15 and 4 days, respectively. The continental slope is between x = 50 and 85 km.

b. Forcing from the upper rise (x = 135 km, y = 187.5 km)

When the source is located on the upper rise, the characteristics of waves are similar to those in the previous case, but energy is higher at the slope–rise junction. Figure 4 shows the energy density and the transport streamfunction at a period of 36 days. Ray paths are in the $-y$ direction along isobaths as in the previous case. Propagation of energy toward the steep continental slope is evident. Energy accumulates at the rise and slope junction. Some energy leaks to the deep ocean. The volume transport of the waves is similar to that in Fig. 2 and is confined to the deep waters. Distribution of depth-integrated kinetic energy is similar to that in Fig. 3.

c. Forcing from the slope (x = 75 km, y = 187.5 km)

Figure 5 shows waves generated by a source on the continental slope at 36 days. Waves are confined mostly to the slope and are weaker than those produced by a source of the same strength on the rise in Fig. 2. Energy propagates in the $-y$ direction along isobaths. Cross-isobath transmission of energy is small. The slope is a wave guide for topographic waves. Transport of TRWs is much smaller than in the case of deep ocean sources. The kinetic energy density and streamfunction for a source at 10 days are shown in Fig. 6. Unlike that in the case of 36 days, the ray path clearly crosses the shelf break onto the shelf. Wave-induced mass transport is also small. Depth-integrated kinetic energy is shown in Fig. 7. Energy maxima at periods of 4, 15 and 36 days are of the same magnitude. Energy of both 15- and 36-day waves decreases rapidly away from the slope, but that of 4-day waves may leak onto the shelf.

d. Forcing from the shelf (x = 45 km, y = 187.5 km)

Figure 8 shows waves generated by a source on the shelf at 36 days. Because the kinetic energy density is large in this case, contour intervals used in this figure are different from other plots. A high energy core is produced near the source. Energy is mostly confined on the continental shelf and decreases sharply across the slope. Two rays are clear in the plot: one toward the coast and one along the shelf break. The steep slope is effective in blocking offshore energy transmission to the rise. In the lower panel, the transport is small and is mostly on the shelf. With decreasing periods, waves become weaker and are less confined by the shelf break.

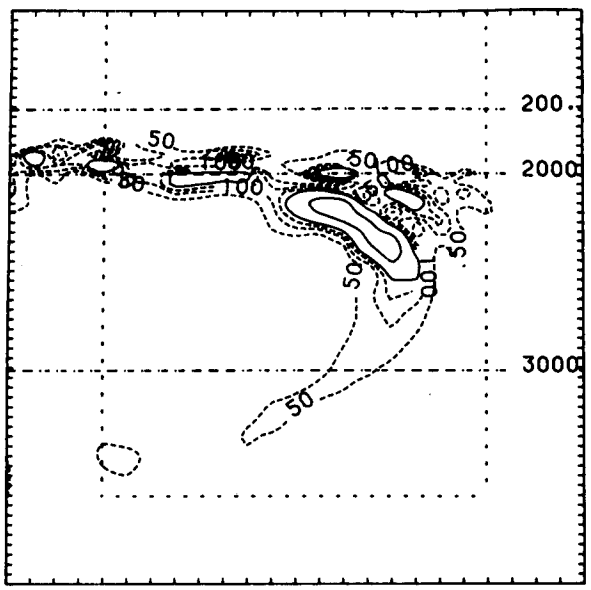

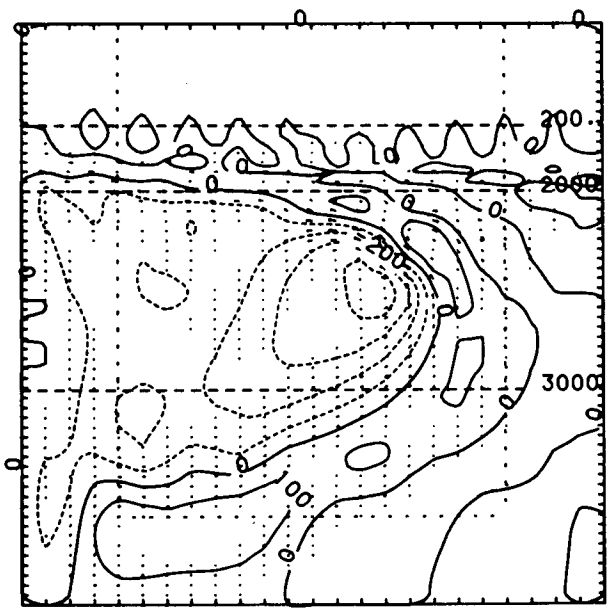

FIG. 4. As in Fig. 2 except generated by a source on the upper rise at 36 days.

Figure 9 shows waves at a period of 4 days. Wave energy now reaches the coast and the shelf break. Some short waves may be found on the slope in the upper panel. These are waves reflected by the $y = 0$ boundary. We will discuss the frictional damping of reflected waves later. Currents associated with the waves are mostly on the shelf and slope.

Offshore distribution of energy in water columns is shown in Fig. 10 for a source on the shelf. Energy maximum is less dependent on wave periods than that in the case of deep ocean sources. At 36 days, little energy transmits through the slope. For waves at 15 and 4

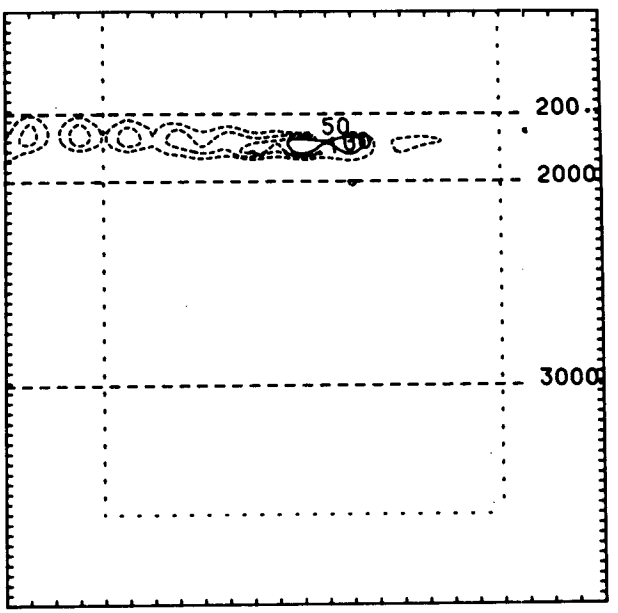

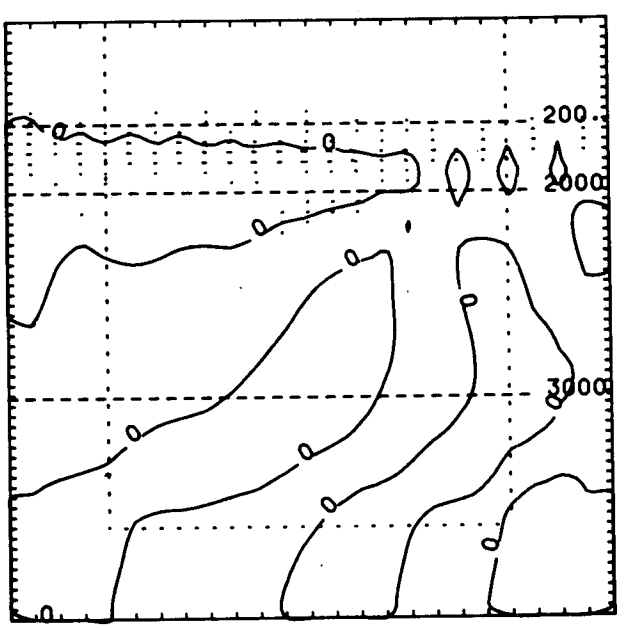

FIG. 5. As in Fig. 2 except generated by a source on the slope at 36 days.

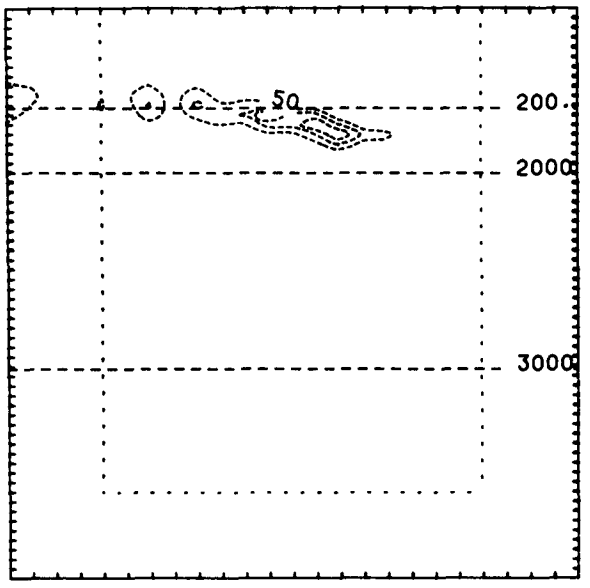

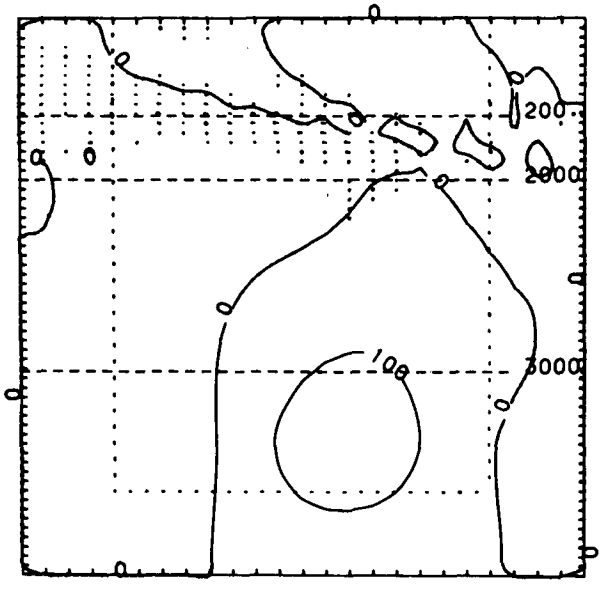

FIG. 6. As in Fig. 5 except generated by a source on the slope at 10 days.

days, wave energy may reach the slope region, but is trapped at the coast. Waves generated are of the characteristics of shelf waves.

4. Effect of friction

To demonstrate that the choice of a frictional coefficient leads to reasonable results, we studied the effect of friction on wave propagation. In the above calculations, a typical frictional coefficient ($r = 5 \times 10^{-4}$ m s^{-1}) has been used. The effect of frictional damping is demonstrated in Fig. 11, where the total kinetic energy in the study region is plotted as a function of r for the 15-day waves. When the source is on the continental rise, total energy increases slowly from $r = 5 \times 10^{-3}$ to 1×10^{-3} m s^{-1}. For r smaller than 5×10^{-4} m s^{-1}, the energy level is nearly constant. On the other hand, energy generated by a source on the shelf is large for r less than 5×10^{-4} m s^{-1}. This high energy level is caused by the ineffectiveness of the model to damp out short waves reflected from the boundaries.

The use of friction in the model is to eliminate unrealistic reflections from open boundaries. The presence of short reflected waves may cause numerical instabilities. In the numerical results with $r = 5 \times 10^{-4}$ m s^{-1}, short waves are effectively eliminated at most periods. Waves are less damped at 4 days on the upper slope, and reflection is not completely eliminated at this period. However, the solutions are not altered drastically by the short waves. The description of the propagation of TRWs should be reasonable.

5. Discussion

The characteristics of waves at periods between 4 and 36 days depend on the parameter $q = r/(\sigma h)$ in (8). This parameter determines the importance of friction on wave propagation. With $h = 4000$ m and $r = 5 \times 10^{-4}$ m s^{-1}, q is much less than one in the above range of wave periods. The frictional force is negligible in the deep waters. The solutions of (8) are slightly damped topographic waves. With $q = 0$, Eq. (8), in terms of velocity components, becomes

$$\frac{\partial v}{\partial x} - \frac{\partial u}{\partial y} - \frac{if}{\sigma} S_x u = \frac{iF_0}{\sigma h}. \tag{9}$$

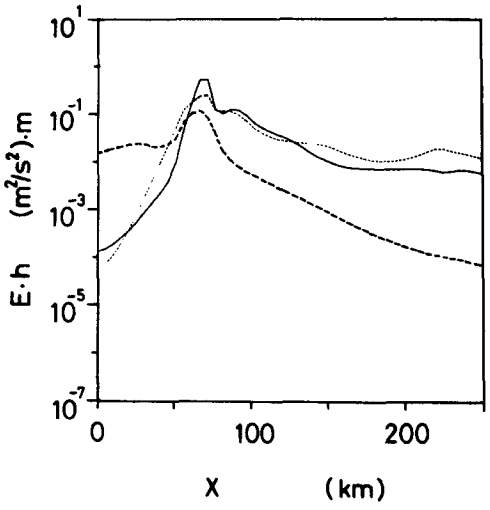

FIG. 7. As in Fig. 3 but generated by a source on the slope.

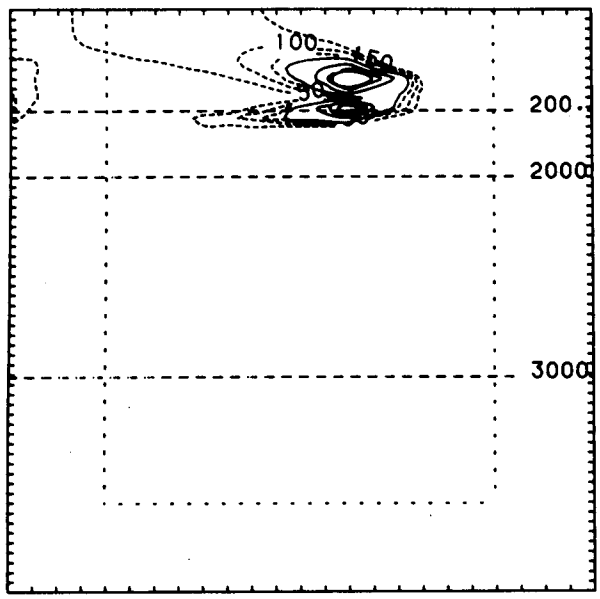

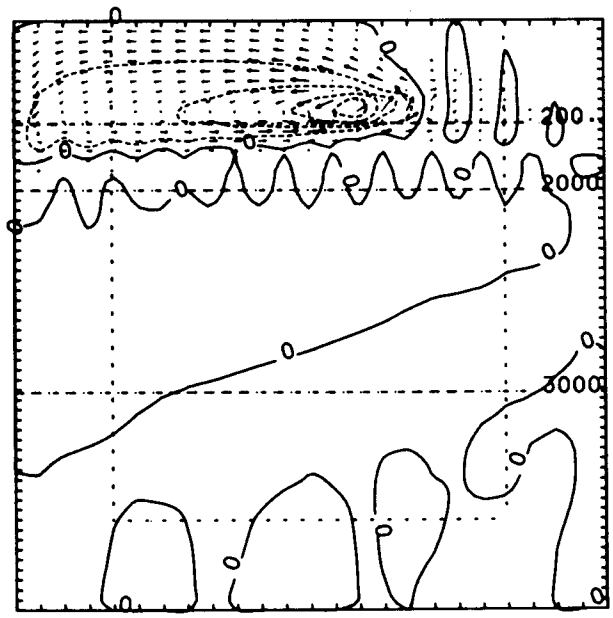

FIG. 8. As in Fig. 2 except generated by a source on the shelf at 36 days. Contour intervals for the dashed and solid lines are 50 and 200×10^{-4} m^2 s^{-2} for kinetic energy. The streamfunction is contoured at 20×10^4 m^3 s^{-1}.

Over the continental rise, S_x is small, and the first term on the left-hand side of (9) balances the forcing term, which is inversely proportional to frequency. This frequency dependence is shown in Fig. 3, in which energy on the rise decreases sharply with periods decreasing from 36 to 4 days. The maximum speeds generated by a source of various periods are summarized in Table 1. On the rise, the maximum speed is from 0.05 to 0.12 m s^{-1} for the 36- and 15-day waves and is much weaker for motions generated by 4-day disturbances. Therefore, high frequency disturbances over the continental rise can hardly generate TRWs.

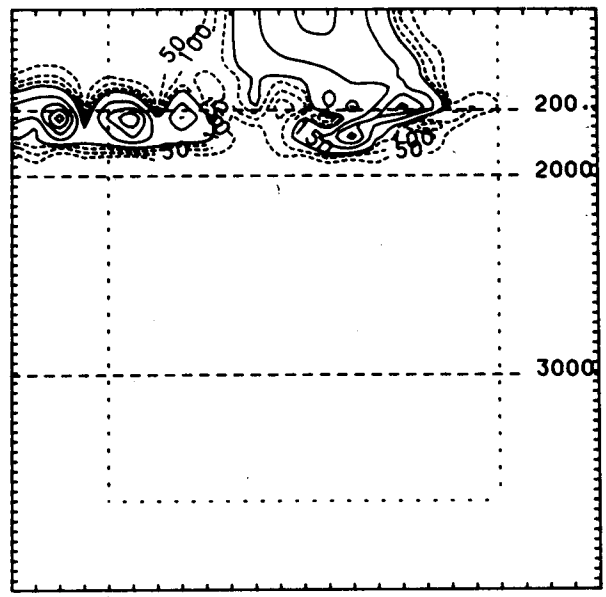

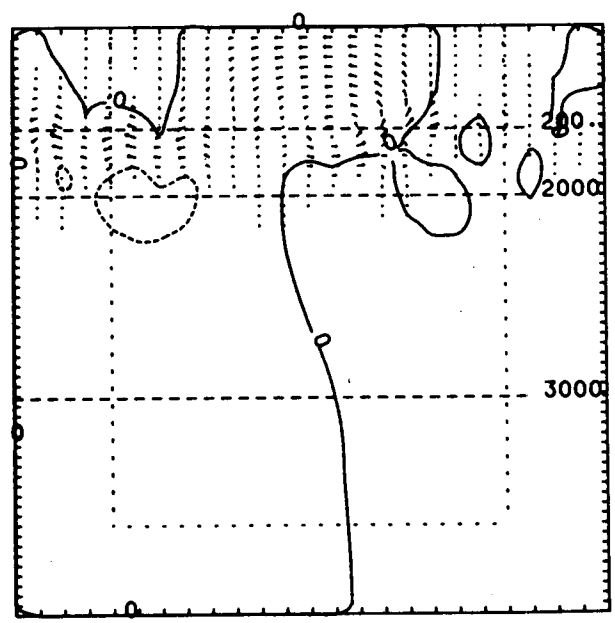

FIG. 9. As in Fig. 2 but generated on the shelf at a period of 4 days.

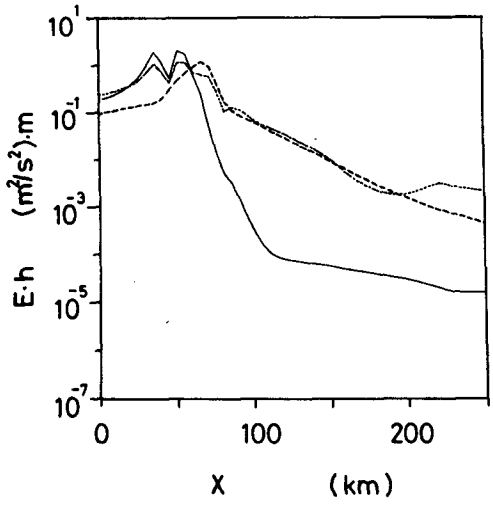

FIG. 10. As in Fig. 3 but generated by a source on the shelf.

When the water depth decreases, q increases, and friction becomes important. The value of q becomes 1 for h = 250 m at 36 days and for h = 30 m at 4 days. Therefore, frictional damping is small for high frequency waves on the upper slope and for waves from 4 to 36 days on the lower slope. For undamped waves on a steep slope, the third term on the left-hand side of (9) balances the forcing term because of large S_x. The resulting equation is independent of frequency. Depth-integrated kinetic energy as shown in Fig. 7 agrees with this expectation. The maximum speed is from 0.06 to 0.09 m s^{-1} for all three wave periods (Table 1).

Over the continental shelf, h is of the order 100 m. The value of q changes from less than 1 for the 4-day waves to about 1 for the 15-day waves and to greater than 1 for the 36-day waves. Therefore, both the 15- and 36-day waves are highly damped waves similar to the solutions of Csanady (1978). On the other hand, the 4-day waves propagate freely. This is the reason why reflected waves are not completely damped out in Fig. 9. This property is seen in Figs. 8 and 9, where the kinetic energy density of the 36-day waves looks like a diffusion plume, but that of the 4-day waves does not. Equation (9) shows that wave strength is inversely proportional to h for undamped waves, and high wave energy may be present for sources on the shelf (Table 1).

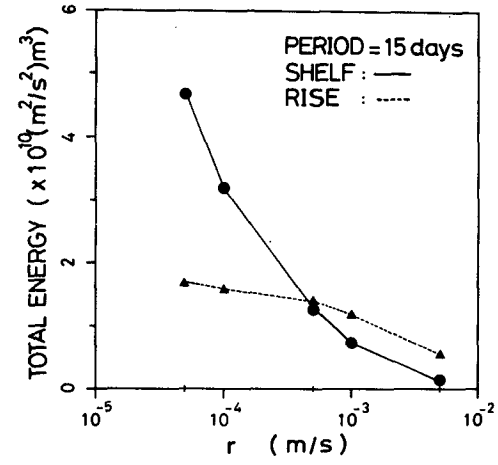

FIG. 11. Total kinetic energy in the study region generated by a source of 10^{-7} m s^{-2}. Forcing is from the shelf (circles) and the rise (triangles), respectively.

TABLE 1. Maximum speed (m s^{-1}) in the study region for different forcing periods and source locations.

	Period (days)		
Locations	36	15	4
Lower rise	0.08	0.05	0.01
Upper rise	0.12	0.09	0.01
Slope	0.09	0.07	0.06
Shelf	0.39	0.40	0.14

6. Shelf–deep ocean interaction

Deep-ocean waves will influence shelf circulation if energy transmission across the steep continental slope is significant. Shaw (1982), Wang (1982), and Csanady and Shaw (1983) have shown that a steep continental slope is a good insulator for steady motions. In the present context, the continental slope is still a barrier to low frequency waves from the deep ocean, but the effectiveness decreases with increasing frequency. At 4 days, the continental slope can no longer block energy propagation from the deep ocean onto the shelf. However, high frequency disturbances are ineffective in generating deep-ocean waves (Table 1). Unless the high frequency source is an order of magnitude stronger than the low frequency ones, deep-ocean waves can hardly influence motions on the continental shelf.

Waves may be generated locally on the shelf and on the slope. The 36-day waves on the shelf are completely confined by the shelf break (Fig. 8). For waves at 15 and 36 days, the steep continental slope is a wave guide. Energy is trapped by the bottom slope (Fig. 5). Louis et al. (1982) have observed that there is a peak on the slope in the offshore distribution of 21-day kinetic energy generated by a Gulf Stream ring (their Fig. 12b) in agreement with our results. Only at 4 days, disturbances may reach the bottom of the slope from the shelf; however, motion is coastally trapped with no offshore energy propagation (Fig. 10). It is evident that deep ocean circulation is not influenced by disturbances on the shelf and slope.

Without the interaction between the shelf and the deep ocean, motions in each region must be generated by local disturbances. In the ocean, alongshore wind

stress is the most important driving force near the coast. Vorticity sources are rare and less effective in generating motions on the shelf (e.g., Shaw, 1982). Therefore, our model may not describe the forcing mechanisms on the shelf. However, the predictions of wave propagation and energy transmission on the slope should be valid independent of the origin of the waves. Our results show that waves on the shelf must be generated by local sources. Because the most important sources on the shelf are in the wind band, energy spectra are high in the high frequency band. On the other hand, only low frequency disturbances are effective in generating deep-ocean waves. Motions on the continental rise are mainly in the low frequency band.

7. Conclusions

Conclusions derived from the numerical results are summarized as follows:

1) Long period waves generated by deep ocean disturbances dominate motion on the continental rise. These waves are refracted and trapped by topography. When sources are not too far away from the continental slope, waves may be observed on the slope before being damped out by friction.

2) At 36 and 15 days, the continental slope is a wave guide for topographic waves, and regions of high kinetic energy density produced by local sources may be found on the slope.

3) Motions on the continental shelf are coastally trapped. High frequency waves on the shelf may be correlated with those on the slope.

4) The continental slope is a good insulator to low frequency waves with periods longer than a week.

Expectations on energy spectrum and coherence can be inferred from the conclusions for current meter observations free from shallow baroclinic noises. Energy spectrum over the continental rise should be high at the low frequency end while that on the shelf should be high in the high frequency band. Also, low frequency disturbances over the continental slope may produce local energy maxima in space. Because energy spectra in the ocean are generally red for periods between a few days and a month, the slope of the spectrum should be steeper on the rise than on the shelf. Coherence between currents over the rise and the lower continental slope should be high in the low frequency band and low near the inertial frequency. On the other hand, high coherence at periods of a few days should be observed in the current data from the outer shelf to the slope–rise junction. Also, high coherence in the along-isobath direction is expected over the continental slope.

Acknowledgments. The authors would like to thank the two reviewers, whose comments greatly improved the manuscript. This work was supported by the National Science Council of the Republic of China under Contract NSC74-0407-M002a-10.

REFERENCES

Bender, C. M., and S. A. Orszag, 1978: *Advanced Mathematical Methods for Scientists and Engineers.* Chapter 10, McGraw-Hill, 593 pp.

Csanady, G. T., 1978: The arrested topographic wave. *J. Phys. Oceanogr.*, **8,** 47–62.

——, and P. T. Shaw, 1983: The "insulating" effect of a steep continental slope. *J. Geophys. Res.*, **88,** 7519–7524.

Gill, A. E., 1982: *Atmosphere–Ocean Dynamics.* Chapter 7, Academic Press, 662 pp.

Hogg, N., 1981: Topographic waves along 70°W on the continental rise. *J. Mar. Res.*, **39,** 627–649.

Kroll, J., 1979: The kinetic energy on a continental shelf from topographic Rossby waves generated off the shelf. *J. Phys. Oceanogr.*, **9,** 712–723.

——, and P. P. Niiler, 1976: The transmission and decay of barotropic topographic Rossby waves incident on a continental shelf. *J. Phys. Oceanogr.*, **6,** 432–450.

Lindzen, R. S., and H. L. Kuo, 1969: A reliable method for the numerical integration of a large class of ordinary and partial differential equations. *Mon. Wea. Rev.*, **96,** 732–734.

Louis, J., and P. C. Smith, 1982: The development of the barotropic radiation field of an eddy over a slope. *J. Phys. Oceanogr.*, **12,** 56–73.

——, B. Petrie and P. Smith, 1982: Observations of topographic Rossby waves on the continental margin off Nova Scotia. *J. Phys. Oceanogr.*, **12,** 47–55.

Ou, H. W., and R. C. Beardsley, 1980: On the propagation of free topographic Rossby waves near continental margins. Part 2: Numerical model. *J. Phys. Oceanogr.*, **10,** 1323–1339.

Peng, C. Y., and P. T. Shaw, 1986: Topographic Rossby waves near the continental margin. *Acta Oceanogr. Taiwan.*, **16,** 61–73 (in Chinese with English abstract).

Rhines, P. B., 1969: Slow oscillations in an ocean of varying depth. Part 1. Abrupt topography. *J. Fluid Mech.*, **37,** 161–189.

——, 1971: A note on long-period motions at site D. *Deep-Sea Res.*, **18,** 21–26.

Shaw, P. T., 1982: The dynamics of mean circulation on the continental shelf. Ph.D thesis. Massachusetts Institute of Technology/Woods Hole Oceanographic Institution, WHOI-82-1, 226 pp.

——, and G. T. Csanady, 1987: Topographic Rossby waves on the continental slope off the east coast of the United States. Submitted to *J. Phys. Oceanogr.*

Thompson, R. O. R. Y., 1971: Topographic Rossby waves at a site north of the Gulf Stream. *Deep-Sea Res.*, **18,** 1–20.

——, 1977: Observations of Rossby waves near site D. *Progress in Oceanography,* Vol. 7, Pergamon, 135–162.

——, and J. Luyten, 1976: Evidence for bottom trapped topographic Rossby waves from single moorings. *Deep-Sea Res.*, **23,** 629–635.

Wang, D. P., 1980: Diffraction of continental shelf waves by irregular alongshore geometry. *J. Phys. Oceanogr.*, **10,** 1187–1199.

——, 1982: Effects of continental slope on mean shelf circulation. *J. Phys. Oceanogr.*, **12,** 1524–1526.

Winant, C. D., and R. C. Beardsley, 1979: A comparison of some shallow wind-driven currents. *J. Phys. Oceanogr.*, **9,** 218–220.